Effects of the nanostructure and nanoporosity on bioactive nanohydroxyapatite/reconstituted collagen by electrodeposition

Keng-Liang Ou,[1]* Jeffery Wu,[2]* Wen-Fu T. Lai,[3,4] Charng-Bin Yang,[5] Wen-Chang Lo,[3] Li-Hsuan Chiu,[6] John Bowley[7]

[1]*Graduate Institute of Biomedical Materials and Engineering, College of Oral Medicine, Taipei Medical University, Taipei 110, Taiwan*

[2]*Department of Oral and Maxillofacial Surgery, Cathay General Hospital, Taipei 110, Taiwan*

[3]*Graduate Institute of Clinical Medicine, College of Medicine, Taipei Medical University, Taipei 110, Taiwan*

[4]*Brain Imaging Center, McLean Hospital, 115 Mill St., Belmont, Massachusetts 02478*

[5]*Department of Orthopedics, Taipei County Hospital, Taipei County 220, Taiwan*

[6]*Graduate Institute of Medical Sciences, College of Medicine, Taipei Medical University, Taipei 110, Taiwan*

[7]*Division of Postdoctoral Prosthodontics, Goldman School of Dental Medicine, Boston University, Boston, Massachusetts 02118*

Received 21 April 2007; revised 24 April 2008; accepted 8 January 2009
Published online 12 March 2009 in Wiley InterScience (www.interscience.wiley.com). DOI: 10.1002/jbm.a.32454

Abstract: Hydroxyapatite (HA)/collagen composites were reported to induce bony growth. Various methods for preparing HA-based composites have been investigated as potential biomaterials for bone substitutes. However, no method can generate a thick nanoporous HA. A novel bone regenerative nanocomposite consisting of nano-hydroxyapatite (HA), nano-amorphous calcium phosphate (ACP) and reconstituted collagen by electrodeposition was designed in this research. Specimens with and without nanoporosity were evaluated using electrochemical measurements, material analyses, and cell-material interactions. The results showed that reconstituted collagen/nano-(HA and ACP) illustrated a multinanoporous structure and enhanced biocompatibility. Nanocomposite was comprised to nano-(HA and ACP) and reconstituted collagen. The core cell structure was formed during electrodeposition. Nanoporosity and nanostructure were observed as formation of nanocomposite. The nano-(HA and ACP) phases were essentially composed of a nanoporous and nanostructural biocomposite. Reconstituted collagen incorporation with the nanoporous and nanostructural biocomposite significantly facilitated the osteogenic differentiation of mesenchymal stem cells. Reconstituted collagen was covered with nano-(HA and ACP), profoundly impacting the enhancement of biocompatibility on application of implant and tissue engineering. The bioactive nano-HA/reconstituted collagen-induced osteogenic differentiation of mesenchymal stem cells enables to enhance bone growth/repair and osseointegration. © 2009 Wiley Periodicals, Inc. J Biomed Mater Res 92A: 906–912, 2010

Key words: reconstituted collagen; electrodeposition; mesenchymal stem cell; nano-hydroxyapatite; nano-amorphous calcium phosphate

INTRODUCTION

Bioceramic materials such as bioglass, aluminum oxide, and hydroxyapatite (HA) are becoming popular as surgical implants and bone grafts in the orthopedic and dental fields.[1–5] Among the bioceramic materials, HA has been extensively applied because of its superior biocompatibility.[6–10] However, as bone substitutes have been for long a subject of intensive investigation, problems of stress shielding due to a mismatching of mechanism properties between the implant and bone are well-known.[8,9] Therefore, stress shielding of the graft and bone

*These authors contributed equally to this work.

Correspondence to: W.-F. T. Lai; e-mail: laitw@tmu.edu.tw or tlai@mclean.harvard.edu

Contract grant sponsor: Cathay Medical Center, Taipei Medical University; contract grant number: TMU-IIC-06

Contract grant sponsor: National Science Council of the Republic of China; contract grant number: NSC93-2314-B-038-038

should be properly resolved. In addition, bone in living tissue constantly undergoes a coupled resorption–reparative process known as bone remolding. HA/collagen composites can induce bony growth into the porous structure, and in sequence HA/collagen composites are biodegradable.[3,11] Previous studies also showed that reconstituted collagen enabled to regenerate bones and joints.[10,12,13] As indicated earlier, numerous procedures for forming HA/collagen composites have been reported,[3,11,14–16] and various methods for preparing HA-based composites have been investigated as potential biomaterials for bone substitutes. Among them, electrochemical deposition is one of the popular methods. However, conventional electrochemical methods *such as anodizaion and sol-gel process* cannot generate HA with a thick (~micrometer scale) nanoporous structure.[14–16] Even though the micro-arc electrochemical method is one of the deposition methods that can form thick porous films, it is not easy to generate nanoporosity. In the micro-arc electrochemical method, film was deposited following high voltage, and resulted in nonisotropic electrodeposition reaction. In addition, high voltage-induced surface damage, including microcracks, was shown following micro-arc deposition.[16] Therefore, the purpose of this study was to employ a new method, electrochemical deposition, which can form a nanoporous HA/reconstituted collagen composite by pulse reverses current density. Specimens with and without nanoporosity were evaluated using electrochemical measurements, material analyses, and cell–material interactions. Bone marrow derived mesenchymal stem cells (MSCs) were selected to evaluate the nanoporous HA/collagen effect on osteogenic differentiation. Scanning electron microscopy (SEM) and calcium assay were employed to assess the osteogenic differentiation from MSCs.

MATERIALS AND METHODS

Materials

Bovine type I collagen was pepsinized and reduced by β-mercaptoethanol. This resulted in α-helix peptides, which were then reconstituted with glutaraldehyde to form a glutaraldehyde polymer-amine complex, which was then redissolved in 5 m*M* acetic acid (HAc).[10,12] HA was prepared as previously described.[3]

Electrochemical deposition

An ASTM F67 grade II Ti sheet with a thickness of 1 mm was used as the substrate. It was cut into discs with a diameter of 14.5 mm for use in the experimental tests. All specimens were mechanically polished using 1500 grit paper and were further polished using 1-μm diamond abrasives. Specimens were finished by applying 0.04-μm colloidal silica abrasives. Before use, all discs were degreased and pre-pickled in acid by washing in acetone and processing through 2% ammonium fluoride, a solution of 2% hydrofluoric acid (HF), and 10% nitric acid at room temperature for 60 s. Finally, all specimens were washed with distilled water in an ultrasonic cleaner. Then, the specimens underwent cathodic polarization at a constant current for 10 min in a 1*M* HF solution at 298 K. The charging current density was varied from 0.1 to 5 A/cm^2. Ti was treated by anodization at a constant current of 15 A/cm^2 for 10 min in a 5*M* NaOH solution to generate the hydroxyapatite layer on the Ti surface. Some specimens were also dipped in NaOH to enable anodized and nonanodized specimens to be compared. A platinum plate was used as a counter electrode in this treatment. The surface morphology of specimens following treatment was analyzed by SEM. The compositions of the films were determined by X-ray photoemission spectroscopy (XPS) using a monochromatic Mg Kα source. The X-ray power was 250 W (15 kV at 16.7 mA). Secondary ion mass spectroscopy (SIMS) was applied to analyze the compositional depth profiles following anodization. An O_2^+ primary ion beam with impact energy of 3 keV was applied. Thin film X-ray diffractometry (TF-XRD) was employed to identify the phases and thus determine the microstructural variations. The incident angle of the X-ray was fixed at 3°. The X-ray diffractometer with Cu Kα radiation was operated at 50 kV and 250 mA. The HA-based microstructure was determined by transmission electron microscopy (TEM). TEM samples with electron transparency were prepared by mechanical thinning followed by ion milling in a precision ion polishing system (PIPS). The early phase of the cell–implant interactions was investigated by performing a morphological analysis of the adhesion, and differentiation of MSCs.

MSC culture and analysis

Consenting bone marrow donors were selected from patients admitted to the Orthopedic Section of Taipei City Hospital, Taipei, Taiwan. None had endocrine disease or was receiving hormone replacement therapy. Bone marrow was obtained from femur fracture site by proximal femur aspiration during surgical treatment procedures. *MSCs* were isolated and cultured in DMEM with 10% bovine serum as previously.[11] Cells were cultured in DMEM incorporated with Nanoporous HA (nHA), and nanoporous HA/reconstituted collagen (nHACOL), respectively. Medium was changed every 2–3 days until subconfluently. The medium was collected for Quantichrom™ calcium assay (BioAssay Systems) for 6 days' cultivation.[17] Samples were diluted and incubated with a phenolsulphonephthalein dye which forms stable blue colored complex specifically with free calcium in the sample. Absorbance was read at 575 nm on a plate reader to determine calcium ion concentration per culture. Six samples were employed for each experiment. Data were analyzed using Student's *t*-test and reported as the mean ± SD. $p < 0.05$ was considered

statistically significant. The cell morphology was further investigated by SEM.

RESULTS

HA with sintering determined by TF-XRD is shown in Figure 1. Only the diffraction peaks of HA and a crystalline structure were found in HA with sintering. HA without sintering yielded diffraction peaks other than those of HA. The diffraction peaks of HA were observed in both HA with and without sintering. In addition, other diffraction peaks were observed in HA without sintering. Namely, HA without sintering consisted of tricalcium phosphate (TCP) phases. TF-XRD analysis indicated the angular dependence of the width at half-maximum, which was used to analyze the variations in grain sizes with surface treatment. The Scherrer equation[18] was used to calculate the mean crystalline size D from the full width at half maximum (FWHM) after correction for the instrumental contribution. The HA grain size without sintering was approximately 55 nm. The HA grain size with sintering was larger after heat treatment at 1000°C or 1200°C for1 h. The HA grain size with sintering were about 135 nm. TF-XRD and TEM investigations indicated that with sintering, HA phases contained extremely fine ACP. The ACP with amorphous structures was formed within the HA matrix after sintering. The coarse ACP then grew into the adjacent HA grains via an electrodeposition reaction. The process of nanocomposite formation by the electroadsorption reaction was defined as ACP + HA + collagen → HA + collagen. When the HA was electrodeposited at 1 ASD, granular particles began to nucleate on the collagen

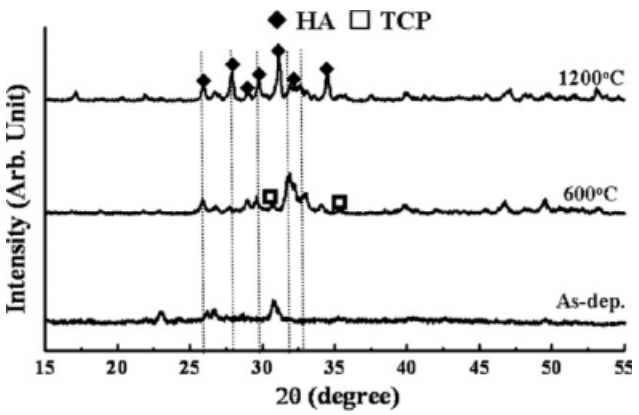

Figure 1. Microstructural variations in hydroxyapatide (HA) with and without sintering as determined by GIXRD. Without sintering, very few diffraction peaks were observed. After sintering, most diffraction peaks were of HA and the structure had become crystalline. The diffraction peaks of tricalcium phosphste (TCP) disappeared.

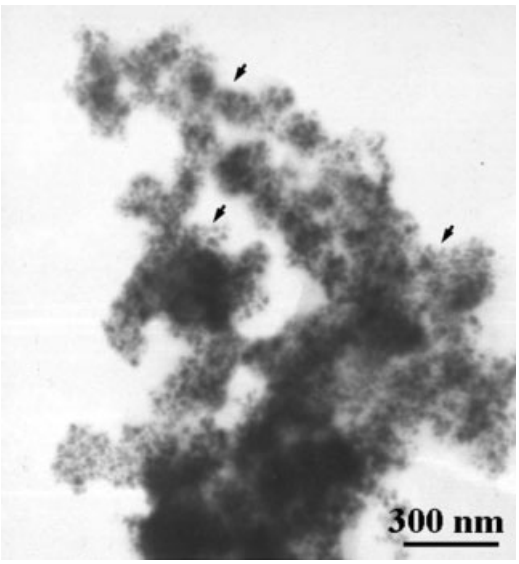

Figure 2. TEM image of the nanocomposite grown on a reconstituted collagen surface. Granular particles were grown and nucleated on the collagen surface. Scale bar represents 300 nm.

surface. Nucleation and growth of HA at the collagen surface were observed (Fig. 2). A dark-field electron micrograph of the fine granular-shaped particles was also obtained. Selected areas of diffraction patterns (SADPs) were also taken from the nanocomposite. From the camera length and *d*-spacings of the reflection spots, the crystal structure of the nanocomposite with coarse particles was determined to be ACP with an amorphous-like structure. The SADPs of the granular-shaped particles revealed that the nanocomposite with nHA was nanopolycrystalline, which showed a closely packed hexagonal structure (not shown). This observation indicates that the microstructure of the nanocomposite was comprised of nano-(HA and ACP) phases. Fine nano-bioceramics underwent phase transformation during the electrochemical reaction.

SEM photographs of collagen, nHA, and nHAc are shown in Figure 3. An appearance of leaf-like sheets with fibers was shown in the collagen [Fig. 3(a)]. A microporous/nanoporous structure was observed on nHA surface, after electrochemical deposition was employed [Fig. 3(b)]. The porous structure was obtained by immersion in a NaOH solution at high temperature for a long period of time.[19,20] Nanoporous structures were also observed on the surface of nHAc as the current density increased up to 5 ASD. The nanoporous structure and multilayer nHAc were observed [Fig. 3(c)]. As widely believed, improved implant performance is attributed to the Ca and P layer, and porosity is due to enhanced adhesion between an artificial bone and the genuine bones. SEM observations indicated that nanocompo-

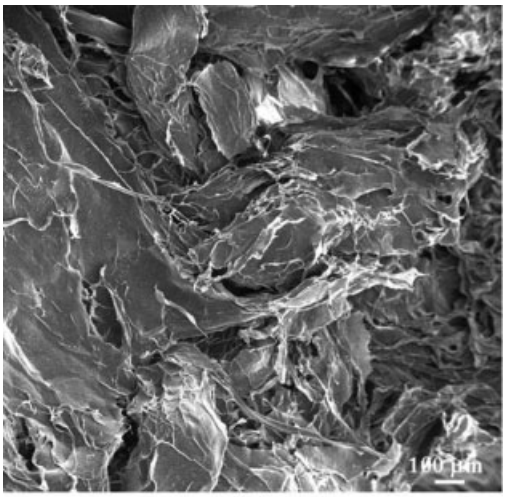

(a)

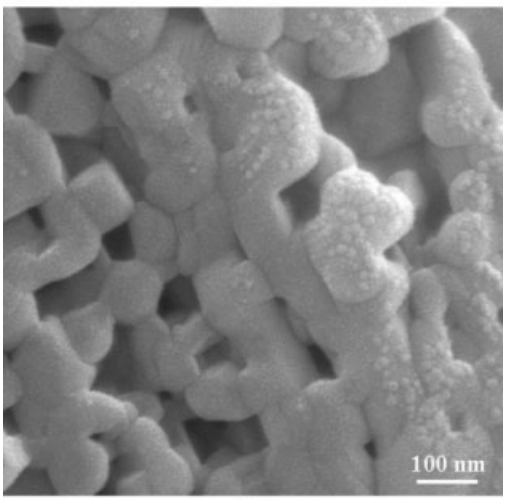

(b)

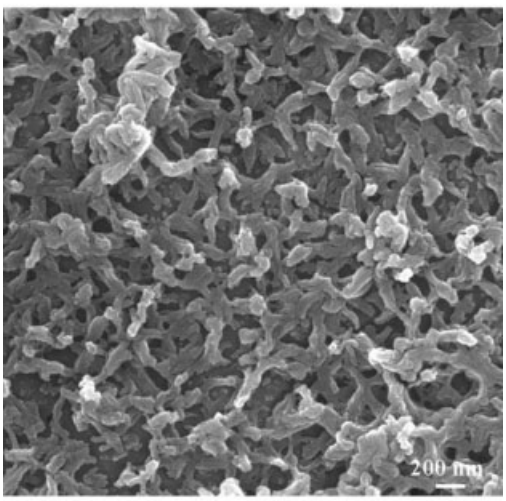

(c)

Figure 3. SEM photographs of collagen without hydroxyapatite (HA), nanoporous HA (nHA), and nanoporous HA/reconstituted collagen (nHACOL). The reconstituted collagen showed a leaf-sheet like structure with fibers in (a). A microporous and nanoporous compsite can be observed on the nHA surface, as shown in (b). Note a thicker nanoporous structure on nHACOL (c).

site materials with multinanoporous layers have higher biocompatibilities.[6–9] These films pretreated in H_2O_2 exhibited enhanced film growth and increased adsorption of plasma proteins.[20] For titanium implants, the thickness of the surface-treated layer increases with time and the concentration of ions (Ca, P, and S) incorporated into the growing oxide from the physiological environment.[21] Therefore, based on the earlier investigation, electrochemically deposited nanocomposites may provide better biocompatibility and osseointegration compared with regular ceramics such as HA.

The atomic statuses of HA and nHAc were further investigated by XPS (Fig. 4). After a survey scan, the Ca 2p high spectra were investigated. In the two bioceramics, the Ca 2p showed two major peaks at binding energies of approximately ~347 and ~351.2 eV. The binding energy peaks correspond to the calcium and phosphate groups that are present in HA's structure.[22] There was little difference in the peaks of HA and nHAc. nHACOL showed relatively broad peaks for Ca 2p, indicating its Ca status slightly differed from that of HA. This is attributed to the low crystallinity and nonstoichiometry of the structure. The position of the Ca $2p_{3/2}$ level clearly shifted from 350.5 to 351.2 eV after electrodeposition. The peak at ~351.2 eV is attributed to the oxygen atoms or molecules that are present at interstitial sites and/or grain boundaries. This phenomenon is also exhibited by titanium prepared by low-temperature plasma treatment.[23] The emission peak at ~351.2 eV from HA and nHACOL dominates the Ca $2p_{3/2}$ binding energy. These results demonstrate that some O atoms do not form strong covalent or ionic bonds

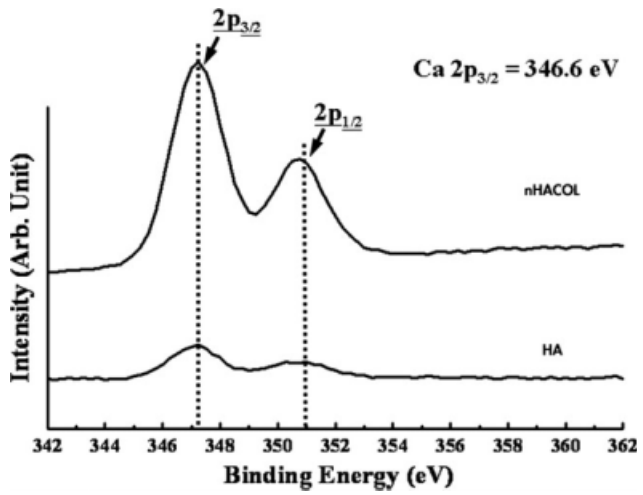

Figure 4. X-ray photoemission spectroscopy (XPS) graph of the chemical atomic status of hydroxyapatite (HA) and nanoporous HA/collagen (nHACOL). After scanning, the Ca 2p high spectra were investigated. In the two bioceramics, the Ca 2p spectra showed two major peaks at binding energies of approximately ~347 and ~351.2 eV.

with Ca atoms during electrodeposition. Some of the introduced O atoms segregate at the interstitial sites and/or grain boundaries in the nanocomposite as a doping material. Electrodeposition strengthens metal-oxygen bonding, revealing that metal oxides are present on the treated surface. The valence states of Ca ions are at the surface, indicating that an O cavity is present under the surface.[9] It was confirmed that a nanoporous and nanostructured oxide layer on the nanocomposite were successfully developed by electrodeposition.

The effect of collagen incorporation with a nanoporous nanocomposite on osteogenic differentiation of MSCs is shown in Figure 5(a–c). Calcium concentration was found higher in culture media of nHACOL group than the nHA group [Fig. 5(a)]. Cells appeared fibroblast-like morphology [Fig. 5(b)] on the nHA, whereas exhibited more spread out filpods [Fig. 5(c)] on nHACOL. It indicated that MSCs were activated and underwent osteogenic differentiation on the surface of collagen with the nanoporous nanocomposite.

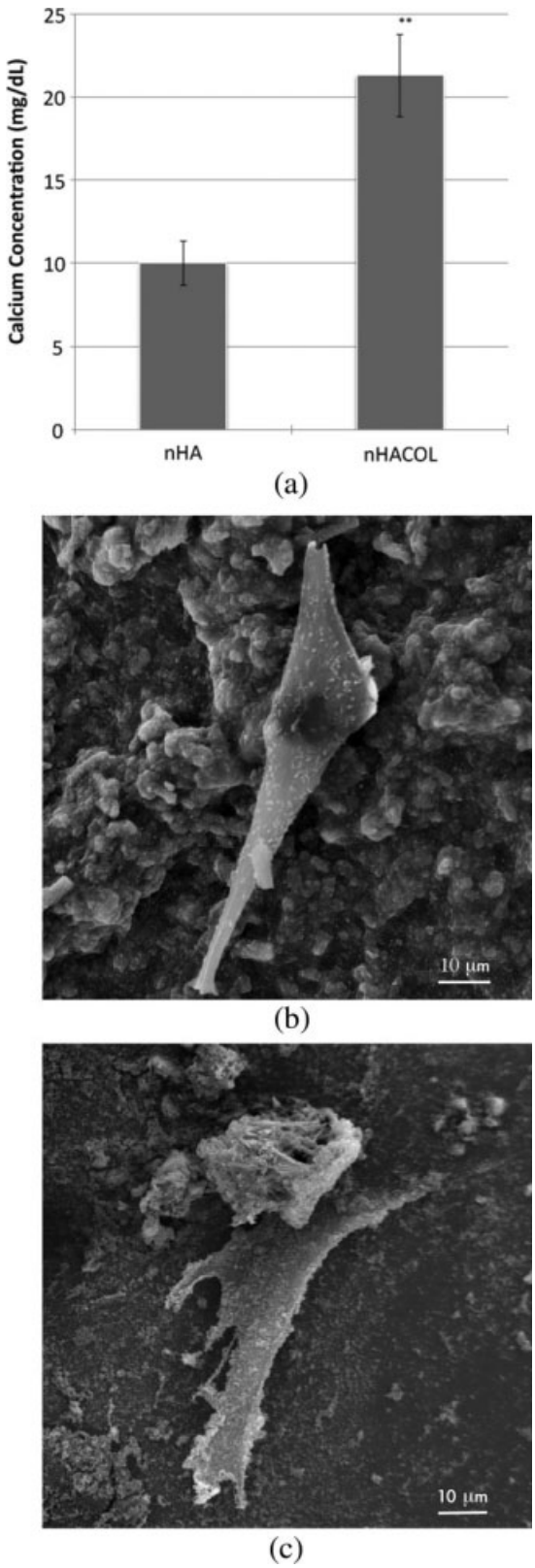

DISCUSSION

Current therapies for bone defect include bone substitute materials such as HA, combined with cell implantation, and/or cytokines. Hydroxyapatite ($Ca_{10}(PO_4)_6(OH)_2$, HA) used previously was constructed as a bone replacement material in restorative dental and orthopedic implants, owing to its physiochemical and crystallographic structure being similar to that of bone mineral.[1,7] Previous researches have also revealed that HA is biocompatible with hard tissue of human beings and exhibits osseoconductive properties.[14,15] Results are still unpredictable[24]; however, primarily due to unsuccessful regeneration of bone extracellular matrix such as collagen, and stress shielding.[8,9] Attempts to increase the efficiency of bone formation and cellular retention, a nanoporous HA/collagen composite was designed in our study. The nHACOL appeared essential for providing mechanical strength for osteoinduction, osteoconduction, and osseointegration.

Figure 5. Medium was collected from each MSC culture incorporated with nHA or nHACOL for over 6 days. A Quantichrom™ calcium assay kit (BioAssay Systems) was used to determine the calcium concentration in the collected culture medium. Samples were diluted and incubated with a phenolsulphonephthalein dye which forms stable blue colored complex specifically with free calcium in the sample. After the incubation the intensity of the color was then measured at 575 nm and calcium concentration was calculated with a standard curve. The data represent means ± SD ($n = 6$) and double asterisk indicates the statistical difference at $p < 0.01$ (a). MSCs were further evaluated cell morphology using SEM image. Cells appeared fibroblast-like cells on nHA group (b), whereas exhibited several spread out filpods on nHACOL group (c).

The use of nanocomposites as bone substitutes is appealing because these substances represent the major inorganic and organic components, constituting approximately 98% of natural bone content.[13] The biocompatibility and osteoconductivity of HA and collagen are well made both materials attractive for orthopedic application.[12–14] Nanocomposites have been proved to be useful as bone substitutes in experimental as well as in clinical settings.[11] It has been presented that a nanocomposite (nanometer size, low crystallinity, and biodegradable HA) shows favorable in vitro and in vivo properties such as bone cell attachment, biodegradation by macrophages, and bone formation.[13,14] Previous study showed more predictable results of nanocomposite (HA/collagen) compared with pure HA or tricalcium phosphate (TCP) in an animal model.[13] The nanocomposite in the present study was nanosize and nanoporous. It was thereby used to be absorbed by the host tissue. The tissue reaction on the various implants should be investigated in the interface of implants. The HA combined with collagen can enhance the behavior of self-setting calcium phosphate bone cements.[14,15] Bone remodeling was also found an increase around HA containing collagen implants in a rabbit model.[3] In this study, the reconstituted collagen showed a leaf sheet-like structure with fibers at lower magnification. At high power, reconstituted collagen appeared a fiber or bundle-like structure and more porous (not shown). In addition, a nanocomposite ceramic containing a porosity and pore structure comes close to the properties of native bone. The porosity and wettability with water and organic solvents will allow loading of the ceramic with drugs such as antibodies and growth factors. A number of alkaline substances were found on the ceramic that can create an alkaline environment inside pores after implantation. This indicates that it may have an impact on factors such as drug stability, solubility, and drug release.

In this study, the reconstituted collagen showed a leaf sheet-like structure with fibers at lower magnification. At high power, reconstituted collagen appeared a fiber or bundle-like structure and more porous (not shown).

Our previous data demonstrated that the limited pepsin-digested collagen reduces immunogenicity of the collagen substrate down to minimal. This limited pepsin-digested collagen remains native α-helix peptides, which were then reconstituted with glutaraldehyde to form a glutaraldehyde polymer-amine complex. The reconstituted collagen acts as an artificial collagen matrix and exhibits a significant inductive regenerative capability.[3,10,12] The induction of regenerative capability was used in our present study. The nHA/reconstituted collagen was designed to mimic a native bone, and exhibits a significant enhancement of osteogenic differentiation by mesenchymal stem cells. Additional *in vivo* studies will be investigated in the future.

CONCLUSION

Nano-(HA and ACP) phases were formed by electrodeposition. Nano-ACP phases were transformed following electrodeposition at high current densities. A nanostructural nanocomposite was formed by adsorption reactions of nano-(HA and ACP) and collagen. The nanocomposite formed by electrodeposition exhibited significant nanoporosity and biocompatibility compared with the HA produced by sintering. Nano-(HA and ACP) play an important role in forming a nanoporous and biocompatible layer on collagen. The phase transformation of ACP and HA was determined during electrodeposition by the field-assisted migration of ion electrolyte systems. This can be explained that the outer layer exhibits a mixed microstructure of amorphous and crystalline ceramics. In conclusion, nano-(HA and ACP) phases are essentially composed of a nanoporous and nanostructural biocomposite. Reconstituted collagen incorporated into the nanoporous and nanostructural biocomposite significantly facilitates the osteogenic differentiation of MSCs. The bioactive nano-hydroxyapatite/reconstituted collagen-induced MSCs' osteogenic differentiation enables to enhance bone growth/repair and osseointegration.

References

1. Lausmaa J, Kasemo B, Mattsson H. Surface spectroscopic characterization of titanium implant materials. Appl Surface Sci 1990;44:133–146.
2. Long M, Rack HJ. Titanium alloys in total joint replacement-a materials science perspective. Biomaterials 1998;19:1621–1639.
3. Lai WF, Deng WP, Tsai YH, Chan WP, Yang WC, Pham W. Japan Patent2002–259518; 2004.
4. Wang XX, Hayakawa S, Tsuru K, Osaka A. Bioactive titania gel layers formed by chemical treatment of Ti substrate with a H_2O_2/HCl solution. Biomaterials 2002;23:1353–1357.
5. Gutensohn K, Beythien C, Bau J, Fenner T, Grewe P, Koester R, Padmanaban K, Kuehnl P. In vitro analyses of diamond-like carbon coated stents: Reduction of metal ion release, platelet activation, and thrombogenicity. Thromb Res 2000;99:577–585.
6. Woo J, Cannon DC: Metabolic Intermediates and Inorganic Ions. ''Clinical Diagnosis and Management by Laboratory Methods'', 17th ed. JB Henry, RA McPherson, Philadelphia, 1984, p 133.
7. Williams RL, Brown SA, Merrit K. Electrochemical studies on the influence of proteins on the corrosion of implant alloys. Biomaterials 1988;9:181–186.
8. Liao SS, Cui FZ, Zhu Y. Osteoblasts Adherence and Migration through Three-Dimensional Porous Mineralized Collagen Based Composite: nHAC/PLA. J Bioact Compos Pol 2004;19:117–123.
9. Huang N, Yang P, Cheng X, Leng Y, Zheng X, Gai G, Zhen Z, Zhang F, Chen Y, Liu X, Xi T. Blood compatibility of

amorphous titanium oxide films synthesized by ion beam enhanced deposition. Biomaterials 1998;19:771–776.
10. Merritt K, Brown SA. Effect of proteins and pH on fretting corrosion and metal ion release. J Biomed Mater Res 1988;22:111–120.
11. Lai WF, Tsai YH, Su SJ, Su CY, Stockstill JW, Burch JG. Histological analysis of regeneration of temporomandibular joint discs in rabbits by using a reconstituted collagen template. Int J Oral Maxillofac Surg 2005;34:311–320.
12. Lai WF. Reconstituted collagen template and the process to prepare the same. US Patent 5876444; 1999.
13. Chen CW, Tsai YH, Deng WP, Shih SN, Fang CL, Burch JG, Chen WH, Lai WF. Type I and II collagen regulation of chondrogenic differentiation by mesenchymal progenitor cells. J Orthop Res 2005;23:446–453.
14. Heimann RB, Schurmann N, Muller RT. In vitro and in vivo performance of Ti6Al4V implants with plasma-sprayed osteoconductive hydroxylapatite-bioinert titania bond coat ''duplex'' systems: An experimental study in sheep. J Mater Sci 2004;15:1045–1051.
15. Wang RZ, Cui FZ, Lu HB, Wen HB, Ma CL, Li HD. Synthesis of nanophase hydroxyapatite/collagen composite. J Mater Sci Lett 1995;14:490–492.
16. Liao SS, Cui FZ, Zhang W, Feng QL. Hierarchically biomimetic bone scaffold materials: Nano-HA/collagen/PLA composite. J Biomed Mater Res Part B 2004;69:158–165.
17. Li LH, Kong YM, Kim HW, Kim YW, Kim HE, Heo SJ, Koak JY. Improved biological performance of Ti implants due to surface modification by micro-arc oxidation. Biomaterials 2004;25:2867–2875.
18. Klug HP, Alexander LE. X-ray Diffraction Procedures. New York: Wiley; 1954.
19. Tanaka SI, Aonuma M, Hirose N, Tanaki T The Preparation of Porous TiO_2 by Immersing Ti in NaOH Solution. J Electrochem Soc 2002;11:D167–D171.
20. Tanaka SI, Aonuma M, Hirose N, Tanaki T. Effect of hydrogen on the formation of porous TiO_2 in alkaline solution. J Electrochem Soc 2002;12:F186–F190.
21. Sundgren JE, Bodö P, Lundström I. Auger electron spectroscopic studies of the interface between human tissue and implants of titanium and stainless steel. J Colloid Interface Sci 1986;110:9–20.
22. Campoccia D, Arciola CR, Cervellati M, Maltarello MC, Montanaro L. In vitro behaviour of bone marrow-derived mesenchymal cells cultured on fluorohydroxyapatite-coated substrata with different roughness. Biomaterials 2003;24:587–596.
23. Lin CC, Cheng HC, Huang CF, Lin CT, Lee SY, Chen CS, Ou KL. Enhancement of biocompatibility on bioactive titanium surface by low-temperature plasma treatment. J Appl Phys 2005;44:8590–8598.
24. Buckwalter JA. Articular cartilage injuries. Clin Orthop 2002; 402:21–37.